Optimization of survivable filterless optical networks exploiting digital subcarrier multiplexing

Mohammad Mohammad Hosseini,[1,*] **João Pedro,**[2,3] **Antonio Napoli,**[4] **Nelson Costa,**[2] **Jaroslaw E. Prilepsky,**[1] **and Sergei K. Turitsyn**[1]

[1]*Aston Institute of Photonics, Aston University, Birmingham, UK*
[2]*Optical Systems Group, Infinera Unipessoal Lda, 2790-078 Carnaxide, Portugal*
[3]*Instituto de Telecomunicações, Instituto Superior Técnico, 1049-001 Lisboa, Portugal*
[4]*Strategy, Architecture, and Engineering, Infinera, Munich, Germany*
*Corresponding author: m.hosseini@aston.ac.uk

In aggregation networks, the traffic patterns resemble hub-and-spoke characteristics, with a few hub nodes connecting several leaf nodes to the outside of the networks. The use of traditional point-to-point transceivers in these applications results in many low-capacity devices at the hub nodes. Optical transceivers leveraging digital subcarrier multiplexing (DSCM) have recently been proposed to support point-to-multipoint transmission in the optical domain, allowing the use of fewer high-capacity devices at these nodes, thus significantly reducing both capital expenditure and operational expenditure. A high-capacity signal comprising multiple subcarriers is transmitted/received at the hub node, while each leaf node has only to transmit/receive the subset of subcarriers that are intended for it, enabling optimization of the type of transceiver used at each node. Broadcasting the optical signal using an optical tree to reach the different leaf nodes, coupled with the possibility of supporting failure survivability, requires developing algorithms to jointly optimize transceiver deployment and the underlying optical trees. This work proposes a novel integer linear programming model for optimizing the design of resilient metro-aggregation networks using DSCM-based coherent transceivers. Results obtained over two realistic mesh networks show that transceiver expenditures can be reduced by a figure between 23% and 44%. © 2022 Optica Publishing Group

https://doi.org/10.1364/JOCN.451182

1. INTRODUCTION

The development of optical networks is a complex technical challenge and requires simultaneous optimization of various solutions with cost and power considerations. Communication service providers (CSPs) are evaluating long-term, sustainable, and profitable solutions in a variety of network segments, ranging from access to metro and core, in order to meet the demands driven by the widespread deployment of 5G services, the advent of the Internet of Things (IoT), the rapid growth of video streaming, and numerous emerging applications. Because different network segments have varying traffic patterns and data rates, the transmission technology, and network design must be tailored to the specific conditions in each segment of the network [1].

The abovementioned growth will be most pronounced for urban networks, which account for a large portion of telecom infrastructure capital expenditures (CAPEX). Hence, adopting technologies that can cost-effectively scale capacity is critical while ensuring high flexibility and reduced operational expenditures (OPEX). In metro-aggregation networks, traffic

to and from a large number of end nodes (leaf nodes) is transmitted from and received by an aggregate node (or nodes) at a central location (hub node). This results in a large imbalance in the amount of traffic handled by the hub and leaf nodes [2]. Point-to-point (P2P) optical transceivers, which transmit and receive data at the same rate at both ends of a link, are used to connect hub and leaf nodes in aggregation networks. As a result, the number of transceivers at the hub node is the same as the sum of all of those at the leaf nodes. This prevents exploiting the reduction in cost, power consumption, and footprint associated with replacing a large number of low-capacity transceivers with a small number of high-capacity ones as proposed in [3]. Given that the metro-aggregation network segment is particularly cost-sensitive [1], the traditional P2P approach hampers the cost-effective scaling of capacity to meet the projected traffic requirements. Alternatively, point-to-multipoint (P2MP) optical transceivers hold the promise of being capable of efficiently coping with the capacity imbalance between leaf and hub nodes. With this approach, a single high-capacity transceiver is located at a hub node, which may be used to broadcast and receive several lower-capacity flows, each of

which can be allocated to a separate leaf node. If such a solution is found to be practicable, it might result in both transceiver cost savings and improved usage of the hub's router/switch.

P2MP optical transceivers were first investigated in [4]. In this application for metro and core networks, data from one or several clients are mapped to several optical channels, with the resulting flows being co-routed and/or individually routed according to the number and location of the end nodes. For instance, the study reported in [5] demonstrates that using a P2MP solution may result in cost savings when 400 Gb/s and 1 Tb/s transponders are used in backbone networks during a five-phase planning period. In [6], it has been shown that sliceable transponders can provide more energy-efficient grooming compared to fixed transponders. Despite these potential savings, the traffic pattern in core and metro-core network segments tends to be more distributed and balanced and, as a result, more naturally supported with P2P transceivers. Moreover, the high capacity required between node pairs means that an entire optical channel (i.e., transceiver pair) is often needed [7].

Recently, a new generation of P2MP coherent transceivers has been introduced [3,8]. It differs from earlier technologies in that it employs digital subcarrier multiplexing (DSCM), a digital communication technology that allows for efficient slicing of the capacity of a single optical channel. The primary advantage of DSCM is that it enables fine granularity [e.g., 25 Gb/s per subcarrier assuming dual-polarization and 16 quadrature amplitude modulation (DP-16QAM) at $\sim$4 GBd] while preserving similar complexity and cost as a P2P transceiver with the same total data throughput. Additionally, improved utilization of router port capacity is achieved through the use of fewer high-capacity interfaces, which reduces footprint and power consumption, and optical layer simplicity is achieved through the use of simpler filterless node designs instead of reconfigurable optical add/drop multiplexers (ROADMs). According to detailed Monte Carlo simulations conducted using realistic network and traffic data from a CSP [8], this novel P2MP solution can result in overall CAPEX savings of up to 76% over five years, assuming a 30% annual traffic increase.

A key characteristic of the DSCM-based P2MP transceivers is that the leaf nodes' lower-capacity transceivers may receive/transmit just the subcarrier (or group of subcarriers) assigned to them. This solution lends itself to being deployed over a fiber infrastructure with intermediate nodes based on simple power split/combine components. These passive optical components are less expensive and less prone to failure than active optical ones. Numerous ways for designing networks using passive optical components have been explored. The concept of a light trail has been proposed in [9,10]. It comprises an architecture and a protocol that enables each source and destination node pair to dynamically establish a lightpath or trail for a specified duration. Optical combiners/splitters perform the add/drop function. A critical aspect when dimensioning filterless networks is that closed loops must be avoided to prevent the same optical signal from traversing the same link twice. Bearing this in mind, the authors of [11] examined the usage of passive components in wide area networks (WANs), which in general can have a mesh physical topology, and how to establish a set of physical optical connections between all

nodes without generating closed loops. Several path protection strategies using wavelength blockers, colored passive filters, and inter-tree transceivers have been investigated in [12]. It has been shown that the use of wavelength blockers and colored passive filters leads to a better cost savings, while the deployment of inter-tree transceivers is slightly more spectrum-efficient. Moreover, the work in [13] studied the optimization of optical tree constructions, routing, and wavelength assignment. However, all these works assumed the deployment of P2P transceivers and did not consider the specific constraints associated with using DSCM-based P2MP transceivers in leaf-and-hub architectures.

In the initial works exploiting DSCM-based P2MP optical transceivers, simple star, chain, and ring network topologies were assumed [3]. Although these topologies are indicative of the majority of aggregation and access networks, the concept can also be applied to metro-aggregation networks, which can be more meshed. Our seminal studies [14,15] present and explore a framework for optimizing routing, modulation format, and subcarrier assignment in mesh networks in order to reduce the overall transceiver cost. However, this optimization framework does not embed the critical constraint imposed by a filterless design, namely, the requirement to avoid optical signal loops. Moreover, complying with these criteria becomes even more challenging when protection against connection failures must be assured. As a result, this article proposes a novel integer linear programming (ILP) model for optimizing the deployment of DSCM-based P2MP interfaces in mesh networks with link protection while maintaining a simple network architecture. This is accomplished by constructing two spectrally disjoint trees using optical splitters/combiners and selectively deploying spectrum blockers and red and blue filters at specific locations to block the full spectrum or a part of it. Also, the incoming link can be terminated at a given node at the local drop.

The rest of this paper is organized as follows. Section 2 describes the P2MP transceiver technology and functionality, and Section 3 details the network architecture and survivable scenario and introduces the reference network topologies. In Section 4, a novel ILP model for jointly optimizing the P2MP transceiver deployment and the underlying optical layer node elements is described. The simulation results obtained for two reference mesh networks are presented and discussed in Section 5. Finally, Section 6 highlights the key findings of the paper and proposes suggestions for future research.

2. POINT-TO-MULTIPOINT ARCHITECTURE

DSCM has been proposed to mitigate the Kerr nonlinear effect in an optical system alone [16] or in combination with digital backpropagation [17]. The first commercial use of DSCM was in high-end P2P coherent line interfaces, with the goal of improving optical performance (i.e., increase in reach) [18,19]. DSCM can also be used to optimize the spectrum, e.g., by adapting it to the current channel, as in the case of a filter cascade [20]. Recently, DSCM was identified as a key enabler for the realization of coherent transceivers that natively support P2MP in the optical domain [8]. Specifically, a high-capacity DSCM-based transceiver generates multiple subcarriers (SCs)

using a single optical source and transmits them to the leaf nodes. This can be accomplished using a broadcast node architecture, where simple optical splitters are used. Each leaf node's low-capacity transceiver processes just the SCs destined for it. In the reverse direction, each leaf node transmits its subset of SCs, and all SCs are optically groomed (e.g., via optical combiners) along the way to reach the receiver at the hub node.

Figure 1(a) shows an illustrative example of a ROADM-based network when P2P transceivers are deployed. Two leaf nodes with traffic requirements of 25G and 100G are considered. Two pairs of 25G and 100G transceivers are needed, and spectrum is allocated only in the required links (i.e., spectrum reuse is possible). In the filterless scenario, which is exemplified in Fig. 1(b), ROADMs are replaced by simpler passive optical splitters/combiners. This simplifies the network architecture and reduces cost but may involve spectrum waste due to the broadcast nature of optical splitters (e.g., the spectrum used by the 100G connection between the hub node and the leaf node closer to it becomes unavailable in the link between both leaf nodes). Importantly, two factors mitigate the importance of spectrum waste in metro-aggregation networks: (i) the lower capacity required in this network segment (compared to core and metro-core networks) means they are far from being spectrum constrained, and (ii) the hub-and-spoke traffic pattern reduces the usefulness of spectrum reuse.

P2MP transceivers can also be deployed with filterless architectures as illustrated in Fig. 1(c). In this case, a 400G transceiver is deployed at the hub node and communicates with the two leaf nodes. In this implementation, it is assumed
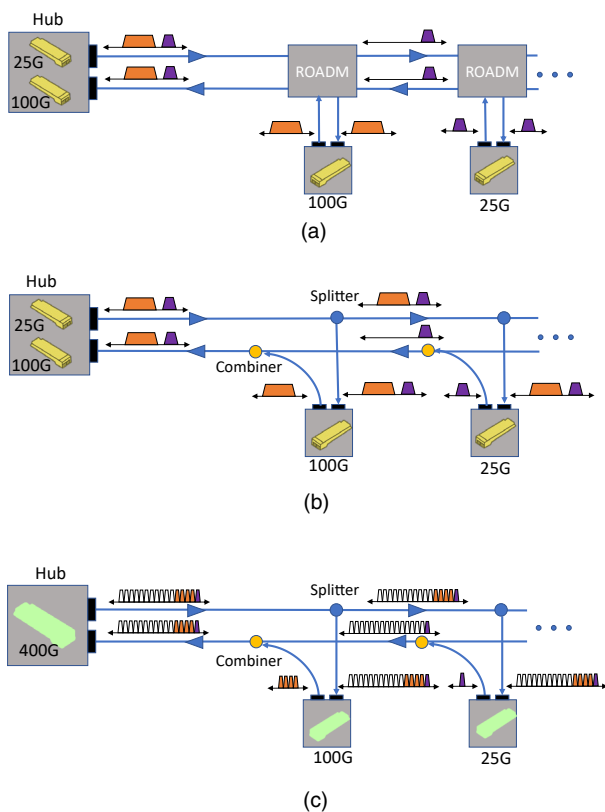
that this transceiver transmits/receives up to 16 SCs, being able to communicate with up to 16 separate leaf nodes. Lower-capacity (lower cost) transceivers are installed at the leaf nodes. The utilization of splitter/combiner elements means that the number of SCs intended for each leaf node can be easily reconfigured as long as the maximum number of SCs each leaf transceiver can handle is not exceeded. For simplicity, in the remainder of this work we consider DP-16QAM when the distance between the hub and leaf nodes is less than or equal to 500 km and DP quadrature phase-shift keying (DP-QPSK) for longer lightpaths (halving SC capacity up to 12.5G, but with the same bandwidth). The symbol rate for each SC is set to 4 GBd. The optical channel formed by the 16 SCs occupies a frequency slot of at least 75 GHz, assuming a frequency granularity of 12.5 GHz. It is worth mentioning that the practicality of DSCM-based P2MP has been shown in both laboratory [21] and field experiments [22].

3. SURVIVABLE NETWORK ARCHITECTURE

Metro-aggregation networks are critical areas of the telecommunications infrastructure. They gather, combine, and route traffic to other network segments with varying degrees of priority, which may be subject to diverse service level agreements (SLAs). Different mechanisms can be used to assure survivability in the face of the most frequent failure scenarios (e.g., fiber cuts) [23]. A widely employed mechanism relies on setting up two disjoint connections between the hub node and each leaf node, designated as the working and the protection connections, and transmitting the same information over both of them. In the event of a failure impacting one of the connections, the service is not disrupted because the traffic is still being transmitted and received over the non-affected connection. In the case of ROADM-based network implementation, link disjointedness of both connections needs to be ensured. On the contrary, suppose the nodes are based on optical splitters/combiners. In this case, two link-disjoint spanning trees can provide full protection since connections only for hub-leaf (but not for leaf-leaf) node pairs are required. However, the necessary but not sufficient condition for having two link-disjoint spanning trees is that the network must have more than $2 \times (N - 1)$ links, where N is the number of nodes. This is unlikely for most ordinary optical networks. Therefore, one way is constructing two spectrally disjoint optical trees by selectively blocking signal transmission partly or fully between certain nodal degrees. This means that the working and protection connections of all leaf nodes have to be considered simultaneously, resulting in a significantly more complex problem to be solved. A multi-tree technique has been proposed in [24] to address the possibility of widespread network failures. The authors suggest a communication protocol based on k rooted spanning trees with the property that the paths between each vertex v and the root are edge disjoint. The two-tree protocol for edges states the following:

- Each leaf node transmits data upward to the root (hub) on both trees.
- When the hub receives data from one of its neighbors, the data are routed downward via both trees.

Fig. 1. (a) P2P transceiver deployment using active ROADM devices. (b) P2P transceiver deployment using passive optical splitters/combiners. (c) P2MP transceiver deployment using passive optical splitters/combiners.

There are three stages involved in locating trees that possess the previously specified attribute. To begin, a depth-first search (DFS) is performed to obtain a DFS numbering, followed by the computation of the $s - t$ numbering [a method of numbering in which all nodes except s (root) and t have adjacent nodes with higher and lower assigned numbers]. Then, using the approaches outlined in [24], the main and backup trees are created. It should be noted that although this method can efficiently find a pair of trees with disjoint paths from leaf nodes to the root, using it when designing a metro-aggregation network based on P2MP transceivers can lead to suboptimal solutions. This is due to the fact that the trees selected can have an impact on the overall quality of the solution (i.e., cost). For example, the paths of a tree may determine which modulation format can be used for SCs being transmitted over that tree, impacting the number and type of transceivers required at the hub and leaf nodes. This observation motivated the investigation of methods to jointly solve the problem of setting up trees with disjoint paths and the problem of routing, modulation format, and SC assignment, having—as a final objective—minimizing the transceiver cost.

As stated above, a key motivation for deploying P2MP transceivers is the possibility of using fewer high-capacity devices at the hub node. It is well known that when the transceiver data rate increases (e.g., between consecutive transceiver generations), the cost increases but not in the direct proportion of the capacity increase [3,25]. This means that the cost per bit/s decreases when opting for a higher capacity transceiver. Therefore, it is usually more cost-effective, if possible, to deploy a smaller number of high-capacity transceivers for the same total aggregate capacity. Figure 2 qualitatively illustrates the relation between transceiver cost and data rate. The red dashed line shows the cost if there were no per bit cost savings when scaling capacity, and possible relative cost figures for three transceivers whose data rate is $4\times$ that of the previous one are also represented. We can model the cost of the transceiver supporting s number of 25G subcarriers with $\text{Cost} = As^B$, where A is a normalization factor for setting the 400G transceiver cost to 1, and B is a positive constant smaller than 1, determining the cost profile. This can be feasible as technology costs tend to decrease exponentially by generations [26]. In this work, two different cost profiles are considered (see Section 5). Using high-capacity transceivers at the hub node involves occupying fewer line ports, so the router or switch installed at this node scales more efficiently, and overall cost, footprint, and power consumption savings can be attained [1].
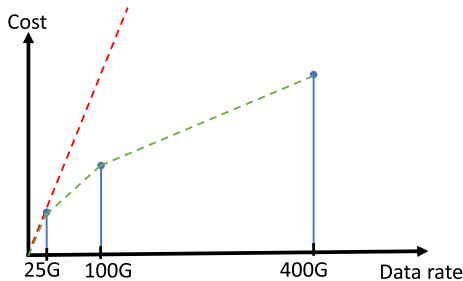

Fig. 2. Visual representation of cost profile versus data rate and possible cost decrease compared to a linear cost scale.

4. OPTIMIZATION FRAMEWORK

The P2MP optimization framework aims to discover the most cost-effective configuration of P2MP transceivers for a given traffic distribution and metro-aggregation network topology, allowing support of link protection and assuming that nodes are based on simple optical splitter/combiner devices. In order to accomplish this goal, we have devised an ILP model. The model's input parameters and decision variables are as follows.

Input Parameters

- $G(V, E)$: network graph with nodes $u, i, j \in V$ and links $l = (i, j) \in E$.
- V^-: a subset of V defining leaf nodes.
- W_{ij}: length of link $(i, j) \in E$.
- $T(u)$: number of 25 Gb/s SCs required by leaf node u. This is assumed to be the maximum required traffic of the downstream and upstream directions.
- L_r: maximum reach with the highest modulation format.
- O_h: a set of transceivers used at the hub node.
- O_l: a set of transceivers used at the leaf nodes.
- C_o: cost of transceiver type o.
- D_o: maximum data rate (with the highest modulation format) of transceiver type o.
- B: very large positive number.

Decision Variables

- x_{ij}^t: 1 if edge $(i, j) \in E$ is selected for tree t; 0 otherwise.
- f_{ij}^t: positive integer variable indicating flow from vertex i to j on tree t.
- y_{ij}^{tu}: 1 if edge $(i, j) \in E$ is in the path from leaf u to the hub on tree t; 0 otherwise.
- M_u^t: 1 if path from leaf u to the hub is longer than L_r; 0 otherwise.
- Δ_o^t: number of transceivers of type o used at the hub on tree t.
- δ_{ou}^t: number of transceivers of type o used at leaf node u on tree t.

The objective of the ILP model is to minimize the total transceivers' cost:

$$z = \sum_t \sum_{o \in O_h} \Delta_o^t \times C_o + \sum_t \sum_{u \in V^-} \sum_{o \in O_l} \delta_{ou}^t \times C_o \quad \textbf{(1)}$$

subject to:

Constructing tree(s)

$$\sum_{(i,j) \in E} x_{ij}^t = N \quad \forall t, \quad \textbf{(2)}$$

$$\sum_j f_{ij}^t - \sum_j f_{ji}^t = \begin{cases} N & \forall t, i = \text{Hub}, \\ -1 & \forall t, \forall I \in V^-, \end{cases} \quad \textbf{(3)}$$

$$f_{ij}^t \leq N x_{ij}^t \quad \forall t, \forall (i, j) \in E, \quad \textbf{(4)}$$

$$f_{ji}^t \leq N x_{ij}^t \quad \forall t, \forall (i, j) \in E, \quad \textbf{(5)}$$

Guaranteeing disjointness of trees

$$\sum_j y_{ij}^{tu} - \sum_j y_{ji}^{tu} = \begin{cases} 1 & \forall t, \forall u \in V^-, i = u, \\ 0 & \forall t, \forall u \in V^-, i \neq u, \text{Hub}, \\ -1 & \forall t, \forall u \in V^-, i = \text{Hub}, \end{cases} \quad \textbf{(6)}$$

$$y_{ij}^{tu} \leq x_{ij}^t, \quad \forall t, \forall u \in V^-, \forall (i,j) \in E, \quad \textbf{(7)}$$

$$\sum_t y_{ij}^{tu} \leq 1, \quad \forall u \in V^-, \forall (i,j) \in E, \quad \textbf{(8)}$$

Counting the number of transceivers

$$BM_u^t \geq \sum_{(i,j) \in E} W_{ij} y_{ij}^{tu} - L_r \quad \forall t, \forall u \in V^-, \quad \textbf{(9)}$$

$$\sum_{o \in O_l} \delta_{ou}^t D_o \leq T(u)[M_u^t + 1] \quad \forall u \in V^-, \forall t, \quad \textbf{(10)}$$

$$\sum_{O_b} \Delta_o^t D_o \geq \sum_u \sum_{o \in O_l} \delta_{ou}^t D_o \quad \forall t. \quad \textbf{(11)}$$

The constraint in Eq. (2) ensures that the size of the trees is equal to the number of leaf nodes [assuming there is no zero traffic load (see Section 5)]. According to the constraint in Eq. (3), N units of flow are distributed by the hub node, and all N leaf nodes receive exactly one unit of flow. Flows can only be on trees not exceeding the maximum amount of flows by the constraints in Eqs. (4) and (5). These constraints create spanning trees by fulfilling the tree criteria via a single commodity approach [27]. Paths between each leaf node and the hub on each tree are calculated by the constraint in Eq. (6), where one unit of flow is generated by node u and passes through other nodes; only the hub receives it. The constraint in Eq. (7) confirms that the paths are contained in the trees, whereas the constraint in Eq. (8) ensures the disjointedness of paths for each leaf-hub pair. The constraint in Eq. (9) determines the highest order modulation format that can be used. M_u^t takes the value of 1 if the length of any path in tree t is longer than L_r. For simplicity, but without loss of generality, we assume that the highest order modulation format—16QAM—is feasible for paths shorter than $L_r = 500$ km. For paths longer than this value, QPSK is used instead, halving capacity and spectral efficiency. By multiplying $M_u^t + 1$ with $T(u)$, the effective number of SCs needed is doubled when the longest path in the tree forces the utilization of QPSK. The constraint in Eq. (10) and the constraint in Eq. (11) count the number of required transceivers per type at the leaf nodes and the hub, respectively. It is assumed that the 4.8 THz of the C-band provides sufficient bandwidth to meet all demands, and the ILP model does not require link capacity constraints. In a simplistic analysis, the capacity bottleneck in tree architectures is the capacity of a single link multiplied by the number of links connected to the hub, which is usually more than 1. However, even a single link can support $64 \times 400G$ transceiver flows (64×75 GHz $= 4.8$ THz), which is much larger than the maximum number of 400G transceivers deployed at the hub in this study (see Fig. 8 below).

If the physical topology is two-edge-connected, it can be shown that two trees can be constructed, offering one redundant disjoint path for every leaf-hub pair [27]. The described

ILP model can also model unprotected scenarios by simply limiting the number of trees to 1.

It is noteworthy that the ILP model can also be adapted to dimension the network using P2P transceivers. In this case, transceiver pairs (operating at the same data rate) must be installed at the leaf and hub nodes. This scenario can be modeled by removing the constraint in Eq. (11) and the first term of the objective function in Eq. (1) and by doubling the second term of this function, which corresponds to the leaf node transceiver's cost.

With respect to the expected computational complexity of the ILP model, the number of decision variables is dominated by the term of $n \times l \times t$, where n represents the number of nodes, l indicates the number of links, and t is the number of trees. Moreover, the number of constraints scales with $t \times (n^2 + n \times l)$. In practice, the run time highly depends on the specific condition of problem inputs such as traffic patterns. Most instances took between 1 and 3 min in the unprotected scenarios, while most took between almost 5 and 15 min in the protected scenarios using a machine with 64 GB memory and a 2.3 GHz CPU (12 cores total). In this work, we utilize the General Algebraic Modeling System (GAMS), which is a high-level modeling system for mathematical optimization, and call the odhCPLEX solver, to create and solve the ILP model [28].

5. RESULTS AND DISCUSSION

This section presents a comprehensive examination of the effectiveness of integrating DSCM-based P2MP transceivers with filterless node architecture over metro-aggregation mesh networks. Figure 3 depicts two network topologies in Spain, which Telefónica has defined in the scope of the FP7 IDEALIST project (details can be found in [29]). We consider these two networks as references to examine the effectiveness of the ILP model described in Section 4, as well as to gain insight into the potential of P2MP transceivers to reduce CAPEX. Topology A has 30 nodes and 51 link pairs, while network D comprises 30 nodes and 53 link pairs.

Transceivers capable of operating at 400G, 100G, and 25G are taken into consideration, assuming that the 400G and 100G transceivers can be used at the hub nodes, whereas the 100G and 25G transceivers can be employed at the leaf nodes. For benchmarking purposes, the utilization of a P2P transceiver configuration is also considered. In this case, only 100G interface pairs can be deployed. In terms of spectrum usage,
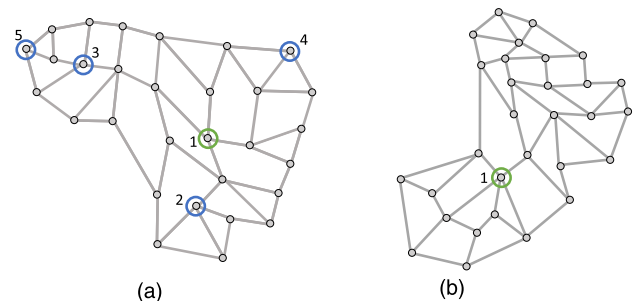
Fig. 3. (a) Topology A and (b) topology D defined by Telefónica.

the outcome of all simulations has been verified to confirm the assumption that enough spectrum holds.

A nonuniform traffic pattern is assumed: the number of 25G capacity each leaf node requires is randomly chosen from the set $[x, x + 4]$, where x takes the value of $\{1, 2, 3, 4, 5, 6\}$ to cover a wide range of traffic load conditions. We utilize the average number of required SCs per leaf node to facilitate readability when displaying the results. All the results shown in the remainder of this section are the average values obtained from 10 independent Monte Carlo runs. Regarding the transceiver cost profiles considered, optimistic and conservative choices are examined to account for cost unpredictability. In the optimistic profile, the cost of a 100G and a 25G transceiver is half and one-fourth of the cost of a 400G transceiver ($A = \frac{1}{4}$, $B = 0.5$), respectively. On the other hand, in the conservative scenario, these values are instead one-third and one-ninth of the cost of a 400G transceiver ($A = \frac{1}{9}$, $B \approx 0.79$).

Figure 4 shows the results obtained considering the optimistic cost profile. Particularly, Fig. 4(a) presents the normalized cost obtained when P2MP transceivers are deployed in topology A for scenarios with and without protection when node 1 highlighted in Fig. 3(a) is the hub node, and the average traffic load varies between 3 SCs and 8 SCs. As expected, the normalized cost is approximately a linear function of the offered traffic in both cases. The cost of interfaces when enforcing protection is slightly higher than twice the cost of the unprotected case. The fraction of cost savings when compared to using P2P transceivers, which are defined as
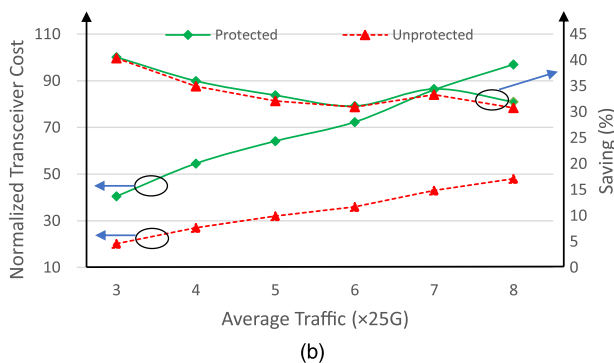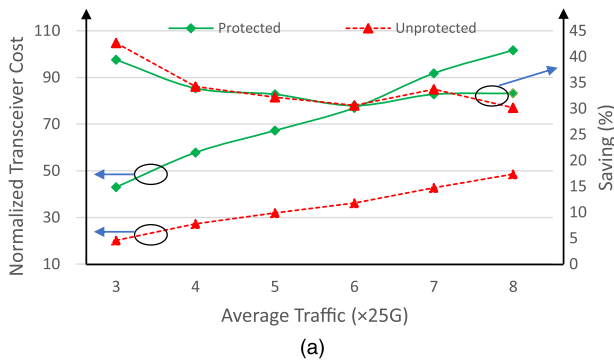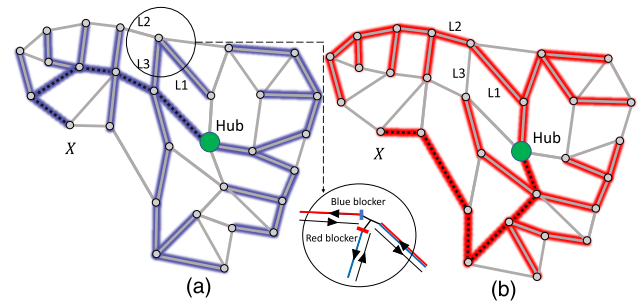

Fig. 5. Example of (a) working and (b) protection trees computed for topology A.

$\frac{\text{Cost}_{P2P} - \text{Cost}_{P2MP}}{\text{Cost}_{P2P}} \times 100$, are also shown in the plot. It can be seen that the amount of savings range between 30% and 44% for both protected and unprotected scenarios. Moreover, it can be observed that the amount of savings is higher for traffic load with an average of 3 SCs. The reason for this is that when average traffic is 3 SCs, a significant number of transceivers deployed are underutilized in P2P scenarios since only 100G transceivers are considered. Hence, for average traffic equal to or below 3 SCs, using 25G transceivers could assist in reducing the cost in P2P scenarios. However, this would also imply using more transceivers at the hub and leaf nodes, leading to a potentially larger footprint and higher power consumption in the router/switch located at these nodes.

Figure 4(b) shows the same set of results but obtained for topology D with node 1 illustrated in Fig. 3(b) as the hub node. Although the number of leaf nodes and the traffic pattern is the same as those in topology A, the normalized P2MP transceiver cost for topology D is slightly lower than that for topology A in the protected scenario, while for the unprotected scenario, it is almost the same. It is important to note that the tree construction is more constrained in protected scenarios since the two trees must meet the conditions stated in Section 3. This fact and the fact that the average link length in topology A is longer than that in topology D can lead to higher utilization of the QPSK modulation format in the former topology, increasing cost. Overall, the amount of transceiver CAPEX saved ranges between 30% and 40% in topology D.

In order to gain insight into the tree solutions found by the ILP model, an instance of the working and protection trees computed for topology A is depicted in Fig. 5. The black dashed lines indicate two disjoint paths from leaf node X to the hub node. Although the working and protection trees might have shared links, the existence of two disjoint paths for each leaf node is guaranteed. In the case of shared links between the two trees, it is assumed that one of the trees uses half of the spectrum, whereas the other half is reserved for the second tree. This strategy can be implemented using red and blue filters, and it is called a semi-filterless solution [30]; however, it maintains the passive feature. In this example, the two trees have 14 shared links, 15 separate links each, and 7 unused links.

For completeness, we also assess the impact of using the conservative cost profile, according to which 400G transceivers are comparatively more expensive than in the optimistic cost profile. Figures 6(a) and 6(b) plot the normalized P2MP

Fig. 4. (a) Normalized P2MP transceiver cost for topology A and corresponding savings compared to the P2P approach and (b) normalized P2MP transceiver cost for topology D and corresponding savings compared to the P2P approach for an optimistic cost profile.
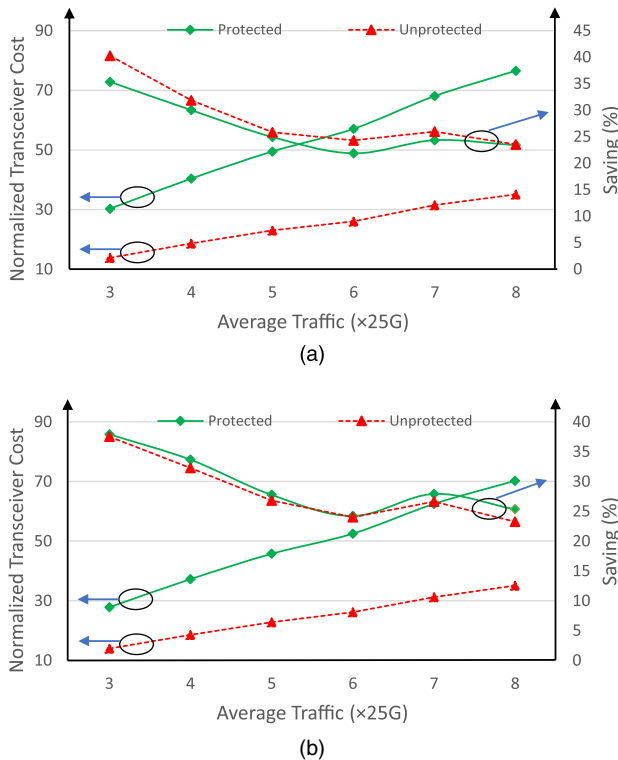
(a)

(b)

Fig. 6. (a) Normalized P2MP transceiver cost for topology A and corresponding savings compared to the P2P approach and (b) normalized P2MP transceiver cost for topology D and corresponding savings compared to the P2P approach for a conservative cost profile.

transceiver cost under the conservative cost profile and the savings when compared to the P2P approach in topology A and topology D, respectively. As can be observed in both plots, the trends are essentially the same as those reported with the optimistic cost profile. However, as expected, slightly smaller cost savings are obtained. In topology A, cost savings range between 24% and 40%, whereas savings between 23% and 38% are achieved in topology D.

The cost savings enabled by P2MP transceivers are a consequence of two key effects:

- High capacity transceivers have a lower cost per bit/s.
- Aggregation of small traffic flows into a single P2MP transceiver and improves utilization.

At low traffic loads, both effects are present, and this explains the larger savings observed in Figs. 4 and 6 for low traffic loads. As the traffic load increases, the second effect has a diminishing impact.

The location of the hub node can affect the total transceiver cost. For instance, having the hub node at a central location, which is the case considered in the previous simulations, should allow the length of the paths used to reach the farthest leaf nodes to be decreased. Nevertheless, the choice of the hub node might be driven by other factors, such as the location of the dominant sources of traffic (e.g., the presence of large data centers) and interfacing with the metro-core network. The impact of different hub node locations is evaluated by considering five possibilities for the hub node in topology A, which
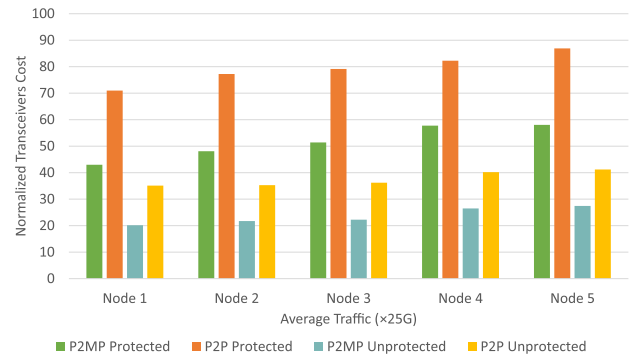

Fig. 7. Normalized transceiver costs for different hub locations in topology A.

are shown in Fig. 3(a). Figure 7 presents the normalized transceiver cost for all five cases, considering the two transceiver types (P2MP and P2P) and whether enforcing link protection or not. The results presented were obtained for an average traffic load of 3 SCs. The highest P2MP transceiver cost occurs when node 5 is selected as the hub, whereas the minimum P2MP transceiver cost is obtained when node 1 is chosen. The cost when using P2P transceivers follows the same trend as that observed with P2MP devices; that is, allocating the hub to a node in the network periphery usually results in higher transceiver cost than when the hub is closer to the center. The cost savings from using P2MP instead of P2P transceivers are between 29% and 42%. Therefore, these results also provide evidence that the cost advantage of using P2MP transceivers is preserved, regardless of the hub location.

The number of transceivers discriminated per rate for protected P2MP and P2P scenarios for topology A and an optimistic cost profile are shown in Fig. 8. In the P2MP scenario, the number of 400G transceivers increases proportionally to the total traffic load. The 100G transceivers also scale with the requirements of leaf nodes, whereas the number of 25G transceivers used is kept at similar levels (only being useful when the usage of 100G transceivers would result in significant capacity underutilization). With P2P transceivers, there is limited ability to simultaneously address the transceiver underutilization problem and hub router footprint waste. Particularly, deploying higher-data-rate P2P transceivers can aggravate the former, whereas deploying lower-data-rate P2P transceivers exacerbates the latter. Conversely, P2MP transceivers enable low-capacity or medium-capacity transceivers at leaf
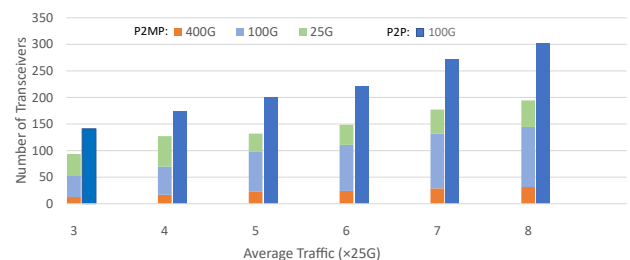

Fig. 8. Number of P2P and P2MP transceivers in the protected scenario versus traffic loads for topology A and an optimistic cost profile.

nodes to be exploited without an increase in line port usage at the hub node.

6. CONCLUSIONS

This paper has described a novel ILP model for optimizing the design of DSCM-based P2MP transceivers in survivable filterless networks. The cost of supporting all traffic requirements using P2MP transceivers was compared to that of utilizing traditional P2P transceivers in two reference network topologies and differing traffic load levels. The results provide evidence that significant cost savings can be achieved, ranging from 23% to almost 44% depending on the average traffic load and the transceivers' cost profile. The savings hold for both protected and unprotected scenarios. Future work will extend the analysis by including more detailed modeling of physical impairments and exploring other potential savings of using P2MP transceivers.

REFERENCES

1. J. A. Hernández, M. Quagliotti, L. Serra, L. Luque, R. L. da Silva, A. Rafel, Ó. G. de Dios, V. López, A. Eira, R. Casellas, A. Lord, J. Pedro, and D. Larrabeiti, "Comprehensive model for technoeconomic studies of next-generation central offices for metro networks," J. Opt. Commun. Netw. **12**, 414–427 (2020).
2. J. Pedro, A. Eira, and N. Costa, "Metro transport architectures for reliable and ubiquitous service provisioning," in *Asia Communications and Photonics Conference and Exhibition (ACP)* (IEEE, 2018).
3. D. Welch, A. Napoli, J. Bäck, W. Sande, J. Pedro, F. Masoud, C. Fludger, T. Duthel, H. Sun, S. J. Hand, A. Mathur, T. A. Eriksson, M. Plantare, M. Olson, S. Voll, and K.-T. Wu, "Point-to-multipoint optical networks using coherent digital subcarriers," J. Lightwave Technol. **39**, 5232–5247 (2021).
4. M. Jinno, H. Takara, Y. Sone, K. Yonenaga, and A. Hirano, "Multiflow optical transponder for efficient multilayer optical networking," IEEE Commun. Mag. **50**(5), 56–65 (2012).
5. V. López, B. de la Cruz, Ó. G. de Dios, O. Gerstel, N. Amaya, G. Zervas, D. Simeonidou, and J. P. Fernandez-Palacios, "Finding the target cost for sliceable bandwidth variable transponders," J. Opt. Commun. Netw. **6**, 476–485 (2014).
6. J. Zhang, Y. Zhao, X. Yu, J. Zhang, M. Song, Y. Ji, and B. Mukherjee, "Energy-efficient traffic grooming in sliceable-transponder-equipped IP-over-elastic optical networks," J. Opt. Commun. Netw. **7**, A142–A152 (2015).
7. J. Pedro, N. Costa, and S. Pato, "Optical transport network design beyond 100 Gbaud [Invited]," J. Opt. Commun. Netw. **12**, A123–A134 (2020).
8. J. Bäck, P. Wright, J. Ambrose, A. Chase, M. Jary, F. Masoud, N. Sugden, G. Wardrop, A. Napoli, J. Pedro, M. A. Iqbal, A. Lord, and D. Welch, "CAPEX savings enabled by point-to-multipoint coherent pluggable optics using digital subcarrier multiplexing in metro aggregation networks," in *European Conference on Optical Communications (ECOC)* (IEEE, 2020).
9. I. Chlamtac and A. Gumaste, "Light-trails: a solution to IP centric communication in the optical domain," in *International Workshop on Quality of Service in Multiservice IP Networks* (Springer, 2003), pp. 634–644.
10. A. Gumaste and I. Chlamtac, "Light-trails: a novel conceptual framework for conducting optical communications," in *Workshop on High Performance Switching and Routing (HPSR)* (IEEE, 2003), pp. 251–256.
11. C. Tremblay, F. Gagnon, B. Chatelain, E. Bernier, and M. P. Belanger, "Filterless optical networks: a unique and novel passive WAN network solution," in *IEICE Proceedings Series* (2007), Vol. 49.
12. M. Ibrahimi, O. Ayoub, F. Albanese, F. Musumeci, and M. Tornatore, "Strategies for dedicated path protection in filterless optical networks," in *IEEE Global Communications Conference (GLOBECOM)* (IEEE, 2021).
13. B. Jaumard, Y. Wang, and N. Huin, "Optimal design of filterless optical networks," in *20th International Conference on Transparent Optical Networks (ICTON)* (IEEE, 2018).
14. M. M. Hosseini, J. Pedro, N. Costa, A. Napoli, J. E. Prilepsky, and S. K. Turitsyn, "Optimized design of metro-aggregation networks exploiting digital subcarrier routing," in *Proceedings of the Asia Communications and Photonics Conference (ACP)*, Shanghai, China, October 2021.
15. M. M. Hosseini, J. Pedro, A. Napoli, N. Costa, J. E. Prilepsky, and S. K. Turitsyn, "Design of survivable metro-aggregation networks based on digital subcarrier routing," in *IEEE Global Communications Conference (GLOBECOM)*, Madrid, Spain, December 2021.
16. M. Qiu, Q. Zhuge, X. Xu, M. Chagnon, M. Morsy-Osman, and D. V. Plant, "Subcarrier multiplexing using DACS for fiber nonlinearity mitigation in coherent optical communication systems," in *Optical Fiber Communication Conference (OFC)* (Optical Society of America, 2014), paper Tu3J.2.
17. F. Zhang, Q. Zhuge, M. Qiu, W. Wang, M. Chagnon, and D. V. Plant, "XPM model-based digital backpropagation for subcarrier-multiplexing systems," J. Lightwave Technol. **33**, 5140–5150 (2015).
18. J. Pedro, N. Costa, and S. Sanders, "Scaling regional optical transport networks with pluggable and integrated high-capacity line interfaces," in *Optical Fiber Communication Conference (OFC)* (Optical Society of America, 2021).
19. H. Sun, M. Torbatian, M. Karimi, *et al.*, "800G DSP ASIC design using probabilistic shaping and digital sub-carrier multiplexing," J. Lightwave Technol. **38**, 4744–4756 (2020).
20. T. Rahman, D. Rafique, B. Spinnler, A. Napoli, M. Bohn, A. Koonen, C. M. Okonkwo, and H. De Waardt, "Digital subcarrier multiplexed hybrid QAM for data-rate flexibility and ROADM filtering tolerance," in *Optical Fiber Communication Conference (OFC)* (Optical Society of America, 2016), paper Tu3K.5.
21. A. Rashidinejad, A. Nguyen, M. Olson, S. Hand, and D. Welch, "Real-time demonstration of 2.4Tbps (200Gbps) bidirectional coherent DWDM-PON enabled by coherent Nyquist subcarriers," in *Optical Fiber Communication Conference (OFC)* (Optical Society of America, 2020).
22. A. Napoli, P. Choiseul, A. Madero, G. Garcia, A. Mathur, J. Bäck, J. Pedro, T. A. Eriksson, W. Sande, A. Chase, F. Masoud, and D. Welch, "Live network demonstration of point-to-multipoint coherent transmission for 5G mobile transport over existing fiber plant," in *European Conference on Optical Communication (ECOC)* (2021).
23. J. Pedro and A. Eira, "Hybrid backup resource optimization for VNF placement over optical transport networks," in *International Conference on Optical Network Design and Modeling (ONDM)* (IEEE, 2019).
24. A. Itai and M. Rodeh, "The multi-tree approach to reliability in distributed networks," Inf. Comput. **79**, 43–59 (1988).
25. J. Bäck, J. Pedro, T. Schaich, A. Napoli, P. Wright, A. Chase, D. Welch, and A. Lord, "Hubbedness: a metric to describe traffic flows in optical networks and an analysis of its impact on efficiency of point-to-multipoint coherent transceiver architectures," in *European Conference on Optical Communication (ECOC)* (IEEE, 2021).
26. The Boston Consulting Group, "Reforming Europe's telecoms regulation to enable the digital single market," https://etno.eu/datas/publications/studies/BCG_ETNO_REPORT_2013.pdf.
27. M. O. Ball, T. Magnanti, C. L. Monma, and G. L. Nemhauser, *Handbooks in Operations Research and Management Science: Network Models* (North-Holland, 1995).

28. M. R. Bussieck and A. Meeraus, "General algebraic modeling system (GAMS)," in *Modeling Languages in Mathematical Optimization* (Springer, 2004), pp. 137–157.

29. FP7 IDEALIST Project, "Elastic optical network architecture: reference scenario, cost and planning," Deliverable D1.1, https://cordis.europa.eu/docs/projects/cnect/9/317999/080/deliverables/001-D11ElasticOpticalNetworkArchitecture.doc.

30. J. Chen, S. Khanmohamadi, F. Abtahi, L. Wosinska, Z. Xu, A. Cassidy, C. Tremblay, P. Littlewood, S. Asselin, and M. P. Bélanger, "Passive wide area network solutions: filterless and semi-filterless optical networks," in *13th International Conference on Transparent Optical Networks* (IEEE, 2011).